Clinics in Oncology

Research Article
Published: 03 May, 2024

Evaluation of the Radiological Characteristic of Agilus Material and Assessing the Fit of 3D Printed Bolus from CT and Structure Sensor Methods

*Wang J[1], Ho YW[2], Lok KH[2], Wenjie W[3] and Cheng CY[4]**

[1]Department of Diagnostic Radiology, The University of Hong Kong, Hong Kong, China

[2]Union Oncology Center, Hong Kong, China

[3]Department of Radiation Physics, Zhejiang Cancer Hospital, China

[4]Department of Clinical Oncology, The University of Hong Kong, Hong Kong, China

Abstract

Three D (3D)-printed boluses have been a research hot spot in recent decades; as such patient-specific boluses can reduce the air gaps between boluses and the patient's skin, thus improving radiotherapy treatment outcomes. In this research, the radiological characteristics of Agilus-30 materials were studied by CT value and the percent depth dose measurement experiments. Moreover, in this research, 3D-printed boluses for Phantom's ear and nose were designed and manufactured through both traditional CT reconstruction method and Structure Sensor Pro scanning method. Through this study, the feasibility of using Agilus-30 as 3D-printed bolus material was demonstrated. And it turned out that the fabrication of 3D-printed boluses using Structure Sensor Pro scanners was initially possible. More importantly, the introduction of user-friendly, portable, and affordable 3D scanning devices in this research also opens up new possibilities for the clinical application of patient-customized medical devices in other medical fields.

Introduction

Cancer is one of the deadliest diseases worldwide [1]. Nowadays, more than 50% of cancer patients require radiotherapy as part of their cancer treatment [2-4]. Currently, Megavoltage (MV) photon beams and MV electron beams are commonly used modalities for external radiotherapy. One of the most distinct features of MV beams is the build-up effect, which results in lower surface doses than maximum doses during radiotherapy. This build-up effect offers a significant advantage in radiotherapy when treating deep-seated tumors. However, it can also lead to reduced target coverage for superficial tumors. To address this challenge, tissue compensators (boluses) are commonly employed on the surface of the patients to enhance target coverage for superficial lesions [5,6].

Nonetheless, applying a commercial flat bolus on irregular surfaces can be problematic as it may result in unwanted air gaps between the bolus and the body surface, subsequently decreasing surface doses. As a result, there is a growing research interest in harnessing 3D printing technology for advancements of patient-specific boluses in radiotherapy, which offers the potential to overcome limitations associated with traditional bolus and improve treatment precision and quality [7-9].

Although extensive research has been conducted on bolus materials, a satisfactory material for 3D printed boluses has not yet been identified. Cheap and easily accessible 3D printing materials such as PLA and ABS have apparent drawbacks as they often adversely affect patient comfort due to increasing stiffness. The flexible, odorless, nontoxic, and transparent soft hydrogel-based boluses tend to lose water quickly and are fragile [10].

Researchers have conducted studies to try to find better ways to design patient-specific boluses. It has been proven that designing boluses with professional 3D scanners, such as the Artec Space Spider optical surface scanner (Artec 3D, Luxembourg) with a published resolution of up to 0.1 mm [11] and HandySCAN™ 300 (Creaform, Canada) with a published resolution of 0.1 mm [12], is acceptable. However, due to the complex operational procedures and regulations of these high-precision instruments, as well as their high cost, it is still necessary and urgent to find a 3D scanning method which is cheaper, accessible, and more convenient for clinical staff to master.

OPEN ACCESS

***Correspondence:**
Chi Yuen Cheng, Department of Clinical Oncology, The University of Hong Kong, Hong Kong, China,

Received Date: *27 Mar 2024*
Accepted Date: *26 Apr 2024*
Published Date: *03 May 2024*

Citation:
Wang J, Ho YW, Lok KH, Wenjie W, Cheng CY. Evaluation of the Radiological Characteristic of Agilus Material and Assessing the Fit of 3D Printed Bolus from CT and Structure Sensor Methods. Clin Oncol. 2024; 9: 2069.

ISSN: 2474-1663

Table 1: Comparison of measured density and density calculated by CT calibration curve of Agilus material.

Agilus-Shore value	Agilus-30	Agilus-40	Agilus-50	Agilus-60	Agilus-70
Average CT value (HU)	109.70	111.20	113.80	117.30	113.90
Average physical mass m (g)	30.024	30.361	30.385	30.531	30.800
Physical density ρ (g/cm^3)	1.112	1.124	1.125	1.131	1.141
Density predicted by CT calibration curve µ (g/cm^3)	1.066	1.067	1.068	1.070	1.068
Error (%)	4.137%	5.071%	5.067%	5.393%	6.398%

In this research, Agilus (Stratasys, Eden Prairie, MN, USA) series materials, which is one kind of commercial photopolymer resin compatible with PolyJet printers [13-15] is studied. Moreover, a new handheld scanning instrument called Structure Sensor Pro (Occipital, Inc., Boulder, CO, USA), releasing in July 2021, designed especially for healthcare demands, which is small-sized (109 mm × 18 mm × 24 mm), cheap (less than 1000 US dollars), and has a published resolution of 1.30 mm, was used to generate the 3D-printed boluses [16].

Materials and Methods

Material analysis

CT value measurement: CT calibration curve was used to convert CT Hounsfield Units (HU) to physical density for dose calculations in treatment planning systems. The accuracy of this conversion is crucial to ensure that dose calculations are accurate [17]. Hence, the first material test was a CT value measurement to check how well the sample material's density can be predicted by the CT calibration curve. In this experiment, five 30 mm × 30 mm × 30 mm Agilus (Stratasys, Eden Prairie, MN, USA) cubes in the following shore value: Agilus-30, Agilus-40, Agilus-50, Agilus-60, Agilus-70 were printed by PolyJet J750 printer (Stratasys, Eden Prairie, MN, USA). The average CT value of each cube was measured by the GE Discovery™ RT CT (GE Healthcare, Milwaukee, WI, USA) and the clinical CT calibration curve was used to predict the density of each cube. The actual density, determined based on weight measured by electronic scale (Type BCE62021-1CEU, Sartorius Lab Instruments, Germany) and dimensions, was then compared to the expected density from CT scan. This comparison can illustrate how well our CT calibration curve predicted the materials' physical density and help to verify whether Agilus-30 has better radiological properties compared to high hardness Agilus materials.

PDD measurement: A further assessment of Agilus-30's radiological properties were performed with Percentage Depth Dose (PDD) measurements. Additional blocks with Agilus-30 material that could be used to do PDD measurements were designed and printed. The blocks are consisted of two 20 cm × 20 cm × 0.2 cm blocks, two 20 cm × 20 cm × 0.3 cm blocks, one 20 cm × 20 cm × 1 cm block, four 20 cm × 10 cm × 2 cm blocks, four 20 cm × 5 cm × 5 cm blocks, two 20 cm × 10 cm × 2.5 cm blocks, two 20 cm × 6 cm × 2.5 cm blocks, one 8 cm × 7 cm × 2.5 cm block and one 13 cm × 8 cm × 2.5 cm block. A hole that fits exactly with the Semiflex Ionization Chamber (Type 31010, PTW-Freiburg, Freiburg, Germany) was designed at a depth of 0.5 cm of the 13 cm × 8 cm × 2.5 cm block, so that the ion chamber could be positioned at a certain depth by stacking the various components in various configurations. The ionization chamber was connected to Unidos Webline Electrometer (PTW-Freiburg, Freiburg, Germany). Ionization measurements were performed using a Varian Edge linear accelerator (Varian Medical Systems, Palo Alto, CA, USA) with 6 MV energy, 200 Monitor Units (MU), 600 MU/min dose rate photon beam and a 10 cm × 10 cm field size. The beam was aimed vertically downward with gantry angle of 0°, and Agilus-30 blocks were placed vertically parallel to beam's central axis.

Phantom study

Air gap measurement: In order to verify whether Structure Sensor Pro, a new hand-held, cheap and easy-to-operate 3D scanning instrument, can be used to design 3D-printed boluses with small errors like the high-precision and high-priced 3D scanning instruments, the phantom study was carried out. Ear and nose were chosen as the targets of our phantom study. The boluses are generated in the following two paths.

In the first path (Figure 1), ET Verification Head Phantom (Brainlab AG, Munich, Germany) was firstly scanned by GE Discovery™ RT CT (GE Healthcare, Milwaukee, WI, USA) and then the 3D model of the phantom was reconstructed with Mimics Innovation Suite 20 medical imaging software (Materialise, Leuven, Belgium). Later, Blender 3D modelling software (The Blender Foundation, Amsterdam, Netherlands) was used to design ear and nose boluses that can be used for 3D printing.

In the second path (Figure 2), the same ET Verification Head Phantom was scanned by Structure Sensor Pro (Occipital, Inc., Boulder, CO, USA) and a 3D model of the phantom was obtained directly. Blender 3D modeling software was then used to design ear and nose boluses for 3D printing as well.

After the nose and ear boluses were printed, they were placed on the corresponding parts of the ET Verification Head Phantom and scanned again by GE Discovery™ RT CT (Figure 3). Medical tape (3M™ Micropore Tape 1530-1) was used to assist with the boluses' placement on the phantom. The CT DICOM data were imported into the treatment planning software (version 16.00.00, Varian Medical Systems, Inc., Palo Alto, CA, USA) for analysis. The Region of Interest (ROI) of the nose and ears was outlined by two experienced medical physicists using Eclipse software, and then the air cavity volumes between the phantom and boluses within the ROI were delineated and calculated by Eclipse software (Figure 4). The surface areas between the phantom and boluses were calculated by the ParaView (Version: 5.11.1, Kitware, Inc. and Los Alamos National Laboratory, USA) software. The average air gaps between boluses and the phantom could be calculated as the air cavity volume divided by the surface areas between the phantom and boluses. Moreover, the maximum air gaps between the phantom and boluses could be measured with Eclipse software by the ruler tool.

CT simulation: In the ROI region of the nose outlined before, a sphere with a radius of 0.75 cm was assumed to be the target volume. And in the ROI region of the ear, the upper part of the ear is delineated as the target volume. To establish consistency of the Planning Target Volume (PTV) for the plan comparison, the PTV was defined in the CT image with Superflab bolus and fused to the other two sets of CT images. The Anisotropic Analytical Algorithm (AAA) was used to develop radiation plans from one anterior field for nose boluses and one horizontal field for ear boluses in the Eclipse radiotherapy treatment planning system (version 16.00.00, Varian Medical Systems, Inc., Palo Alto, CA, USA). 6 MV photon beams were used in all plans. The prescription dose was set as 200 cGy of the target volume in the plan. Then the treatment plan was normalized by two experienced medical physicists so that 95% of the target volume could achieve the prescription dose (V95%=100%). Dmax (maximum dose), Dmean (mean dose), Dmin (minimum dose), D95% and D90% (doses that cover at least 95% and 90% of the target volume, respectively), and V95% (volume receiving at least 95% of the prescribed dose) were estimated for all the above cases.

Results

Material analysis

CT value measurement: The results of the CT value measurement experiment and physical density calculation of different Agilus compounds were displayed in Table 1 and Figure 5.

PDD measurement: The result of PDD measurements experiment was shown in Figure 6. The water commissioning PDD curve and TPS modeled PDD curve were imported as comparison to demonstrate how the measured Agilus-30 PDD behaved similarly to water and treatment planning systems.

Phantom study

Air gap measurement: Calculation results of average air gap and average max air gap between different boluses and phantom within ROI are shown in Table 2, 3.

CT simulation results: TPS results of the dosimetric parameters of different boluses are shown in Table 4. Dose distributions and isodose lines corresponding to the radiation therapy plans with different boluses are shown in Figure 7. Dmax, Dmean, and Dmin refer to maximum dose, mean dose, and minimum dose respectively in PTV, D95% and D90% refer to doses that cover at least 95% and 90% of the target volume respectively. V95% refers to volume receiving at least 95% of the prescribed dose in PTV.

Discussion

Material analysis review

According to the CT value experiment, the Agilus-30 block's density was most reliably predicted by the CT calibration curve, among other Agilus components with higher shore values. It is shown that the errors between the densities predicted by CT and the physical density of Agilus-30, Agilus-40, Agilus-50, Agilus-60, and Agilus-70 materials are respectively 4.137%, 5.071%, 5.067%, 5.393% and 6.398%.

What's more, according to the PDD measurement experiment, it can also be seen from Figure 6 that the measured Agilus-30 PDD values keep close to the commissioning water curve in general, which reveals that the radiological property of Agilus-30 material is remarkably similar to that of water. Plus, the calculated doses from the treatment planning system and the measured doses agreed well. This is advantageous for preserving electronic equilibrium at the skin's surface and for dose calculation when using as bolus material. It is also noticed that when the thickness of Agilus-30 material was greater than 5 cm, the deviation of Agilus-30's measured doses from the TPS calculated dose curve and commissioning water curve slightly increased. However, it is acceptable that the PDD of measured Agilus-30 will deviate more from the TPS calculated dose curve and water commissioning curve at deeper depths, as the thickness of boluses commonly used in clinical is only 2 mm to 15 mm [18,19].

In addition, due to the translucent nature of Agilus-30 material, the accurate and reproducible clinical placement of boluses could be confirmed by the clinical staff, which is an advantage that many other 3D printing materials do not have.

However, it is found that the 1 cm thick commercial Superflab bolus is much softer, stickier and more malleable than the 1 cm thick Agilus-30 material. The Superflab bolus can be tightly attached to the surface of the phantom with medical tape in a protruding and flat structure like the bridge of the phantom's nose because of its better ductility, adhesion and softness, while the 3D-printed boluses with Agilus-30 material cannot be deformed by the external force exerted by the medical tape to fully fit the bridge of the nose. But the commercial Superflab bolus is still not malleable enough to fit the more detailed structure in the corneal area, such as the tip of the nose and the pinnae, even with the help of medical tape. Hence, in the nose part, 3D-printed boluses even have larger average air gaps between boluses and phantom than the commercial Superflab bolus while the average max air gaps between phantom and boluses can be reduced by 3D printing technology. And in the ear part with finer structures, both average air gaps and average max air gaps can be reduced by 3D

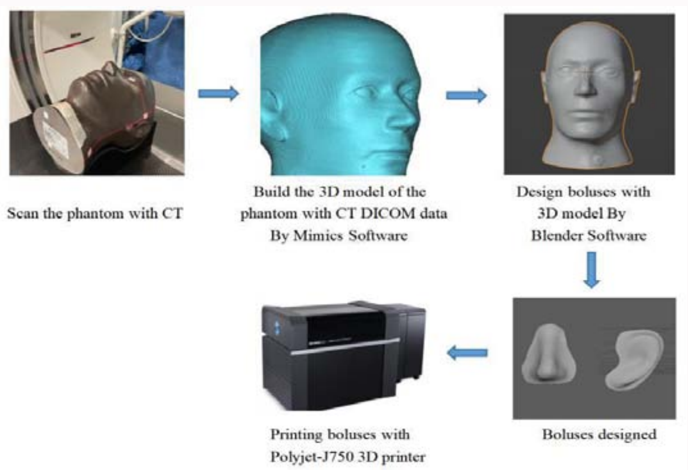

Figure 1: Flowchart of generating boluses from CT reconstruction method.

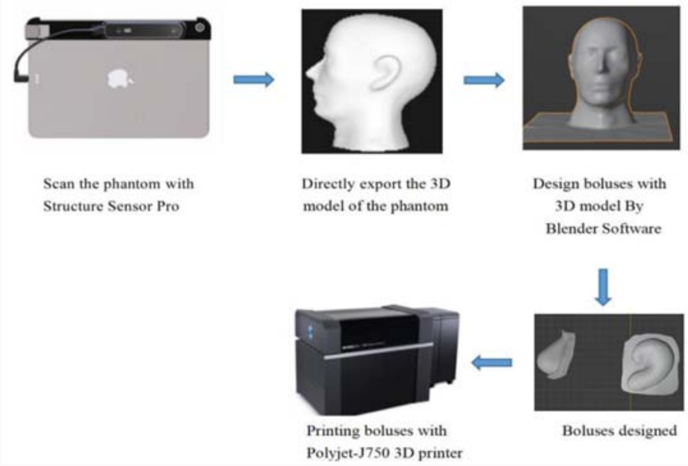

Figure 2: Flowchart of generating boluses from Structure sensor Pro scanning method.

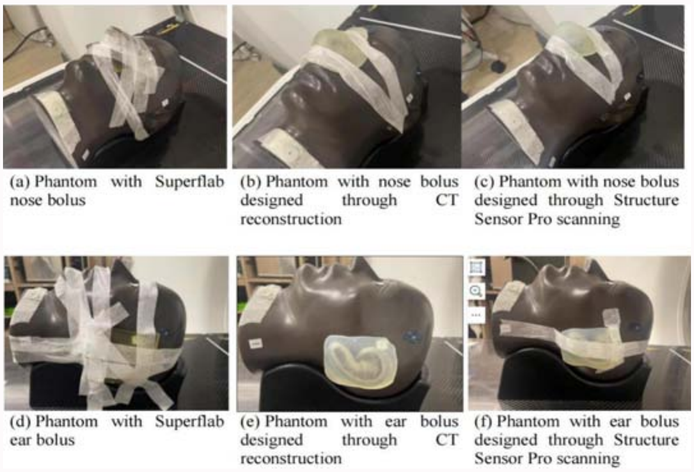

Figure 3: Plot of phantom with boluses.

printing technology.

Moreover, to be further utilized in clinical settings, bolus materials must successfully pass biological testing. Additional biological tests should be held in the future research.

Comparison of CT reconstruction method and structure sensor pro scanning method to make boluses

According to Table 2, average air gaps between commercial Superflab nose bolus, CT reconstructed nose bolus, Structure Sensor Pro scanned nose bolus and phantom within the ROI are 0.868 mm, 0.900 mm, and 0.932 mm respectively. And average air gaps between commercial Superflab ear bolus, CT reconstructed ear bolus, Structure Sensor Pro Scanned ear bolus and phantom within the ROI are 1.818 mm, 0.477 mm, and 1.535 mm respectively. Through this set of data, it is obvious that in the nose part, 3D-printed boluses cannot reduce the average air gaps between boluses and phantom. But in the ear part, the average air gaps between the phantom and 3D-printed ear bolus produced by Structure Sensor Pro scanning method can be reduced by 15.56% compared with the commercial Superflab boluses. And the 3D-printed ear bolus produced by CT reconstruction method could even be reduced by 73.76% compared with the commercial Superflab boluses.

According to Table 3, average max air gaps between commercial Superflab nose bolus, CT reconstructed nose bolus, Structure Sensor Pro scanned nose bolus and phantom are 5.97 mm, 2.80 mm, and 3.70 mm respectively. And average max air gaps between commercial Superflab ear bolus, CT reconstructed ear bolus, Structure Sensor Pro Scanned ear bolus and phantom are 9.20 mm, 2.43 mm, and 5.73 mm respectively. Through this set of data, it can be pointed out that the max air gaps between the phantom and 3D-printed nose bolus produced by Structure Sensor Pro scanning method can be reduced by 38.02% compared with the commercial Superflab bolus. And the 3D-printed nose bolus produced by CT reconstruction method can be reduced by 53.10% compared with the commercial Superflab nose bolus. In the ear part, the max air gaps between the phantom and 3D-printed ear bolus produced by Structure Sensor Pro scanning method and CT reconstruction method can be reduced by 37.72% and 73.59% respectively compared with the commercial Superflab bolus.

Generally speaking, the 3D-printed boluses produced by CT reconstruction method have a better result than the 3D-printed boluses produced by Structure Sensor Pro scanning method. The maximum air gap manufactured by CT reconstruction method in our research is 3.7 mm. This result is consistent with other studies of CT reconstructed 3D-printed boluses showing that the maximum air gaps are within 2 mm to 4.7 mm [11,13,20,21]. The maximum air

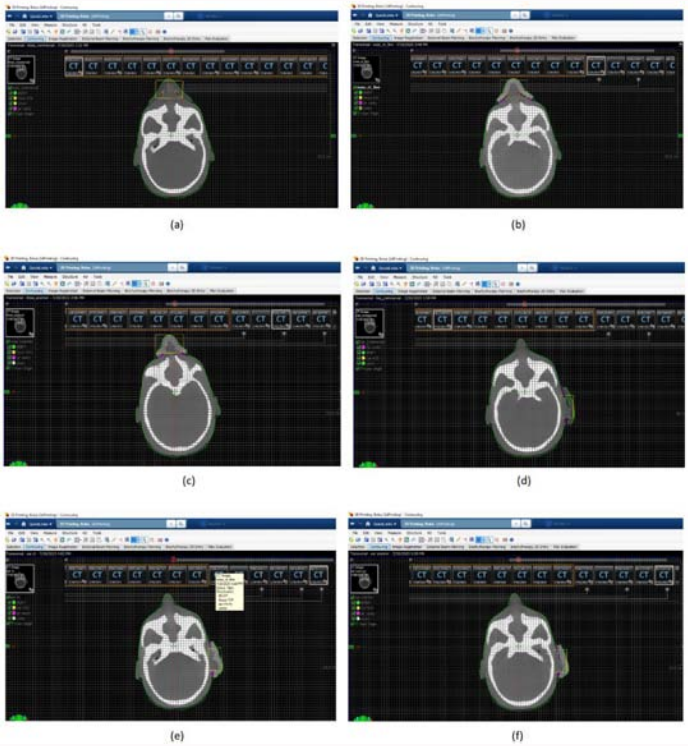

Figure 4: CT slices in TPS showing the ROI (areas inside the yellow line), the air cavities between phantom and different boluses (areas inside the pink line), and the volume of air cavities within the ROI (Union region) with different boluses.

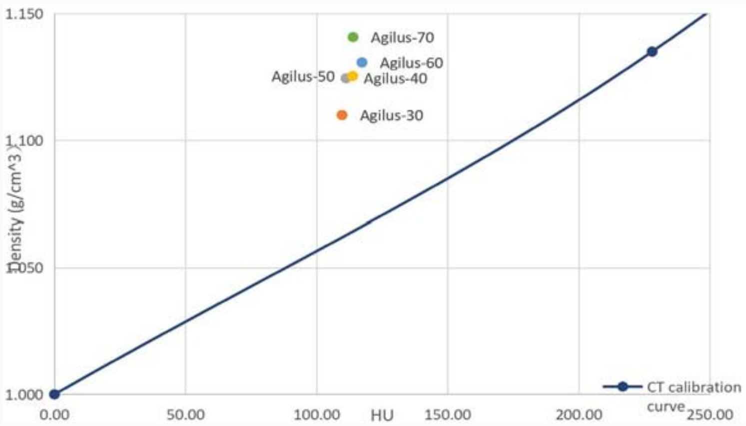

Figure 5: Plot of HU and the measured density for Agilus cube samples and the CT calibration curve.

gap manufactured by Structure Sensor Pro scanning method in our research is 6.8 mm. This result is not as good as other experiments using high resolution 3D scanner to make 3D boluses showing that the maximum air gaps are less than 0.6 mm [11,21].

However, errors introduced in the scanning process cannot be ignored because the Structure Sensor Pro 3D scanner was performed in a non-standardized indoor location. The light and background objects during the scanning operation and the stability of the scanning operator's operation may bring relatively large errors to the scanning process. Because Structure Sensor Pro has a published resolution of 1.30 mm, it is believed that there is still much room for improvement in the experimental results of manufacturing 3D-printed boluses through Structure Sensor Pro scanning.

What's more, the geometric accuracy and reproducibility of printed boluses also depends on the errors introduced at each step of the 3D printing process, from scale uncertainty when converting file formats from DICOM to STL, image segmentation and subsequent modification of the segmented model to printing and post-processing. Therefore, it is believed that the theoretical accuracy and the degree of fit of 3D-printed boluses with phantom will be higher than the results obtained in this experiment.

According to the CT simulation experiment, all the boluses including commercial Superflab boluses and 3D-printed boluses generated by two different methods allow the prescribed dose to be efficiently delivered to the target volume. Overall, the treatment planning results of different boluses were not much different. This is consistent with the results of other similar studies [18,22,23]. And according to this research, 3D-printed boluses could slightly increase

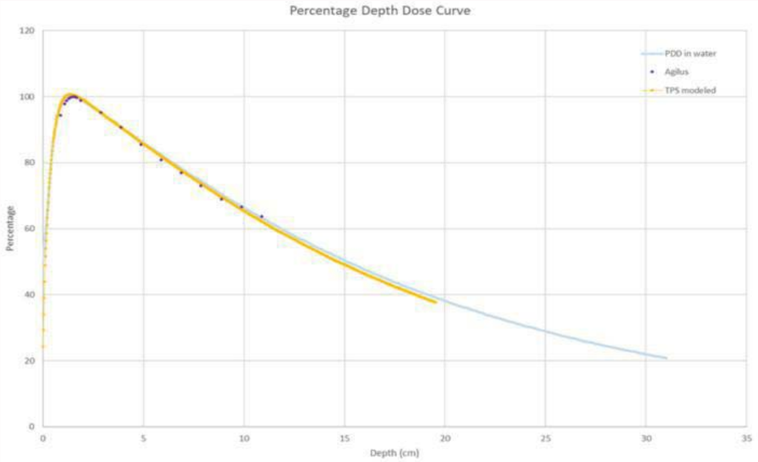

Figure 6: Plot comparing the water commissioning curve (blue line), the TPS modeled PDD curve (yellow line) and the measured PDD (purple dots) of Agilus 30 material.

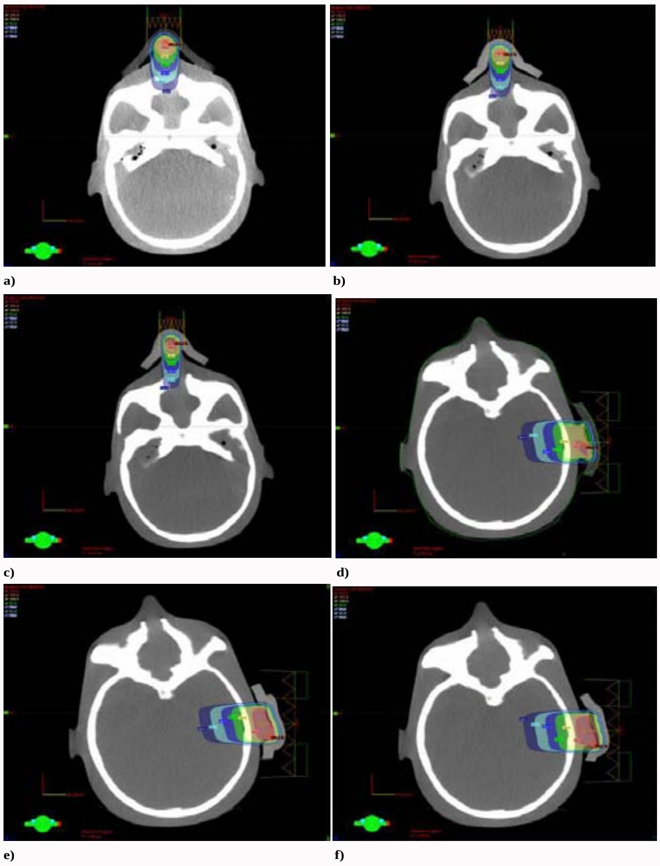

Figure 7: Dose distributions and isodose lines corresponding to the radiation therapy plans with different boluses.

the mean dose delivered to PTV, which is one of the advantages of 3D-printed boluses. It is also proven that the 3D-printed boluses can improve the reproducibility of setup conditions.

Based on above analysis, it is believed that the following research of patient-specific 3D-printed boluses remains beneficial and potential to patients and medical staff for radiotherapy treatment.

Acknowledgment

This Study was funded by the Union Oncology Center and supported by U3DP Lab of The Hong Kong Polytechnic University. The sponsors or funders play no role in the study design, data collection and analysis, decision to publish, or preparation of the manuscript. The authors declare that they have no known competing financial interests or personal relationships that could have appeared to influence the work reported in this paper. The authors declare that they are not involved in the editorial review or the decision to publish this article.

Table 2: Calculation result of average air gap between different boluses and phantom.

Area	Bolus	Total Air Cavity Volume V_0 (mm^3)	Surface Area A_0 (mm^2)	Average air gap (mm) = V_0/A_0
Nose	Superflab bolus	2700	3112.16	0.868
Nose	CT reconstructed bolus	2800	3112.16	0.900
Nose	Structure Sensor Pro scanned bolus	2900	3112.16	0.932
Ear	Superflab bolus	12200	6709.99	1.818
Ear	CT reconstructed bolus	3200	6709.99	0.477
Ear	Structure Sensor Pro scanned bolus	10300	6709.99	1.535

Table 3: Calculation result of average max air gap between different boluses and phantom.

Area	Bolus	Max air gap (mm) at y= -6.25	Max air gap (mm) at y= -4.75	Max air gap (mm) at y= -7.50	Average max air gap (mm)
Nose	Superflab bolus	4.3	4	9.6	5.97
Nose	CT reconstructed bolus	3.3	3.7	1.4	2.80
Nose	Structure Sensor Pro scanned bolus	3.8	4.1	3.2	3.70
Ear	Superflab bolus	9	7.6	11	9.20
Ear	CT reconstructed bolus	1.7	3.1	2.5	2.43
Ear	Structure Sensor Pro scanned bolus	6.8	6.3	4.1	5.73

Table 4: Comparison of the dosimetric parameters of different boluses.

Parameter	Super-flab nose bolus	CT Reconstructed nose bolus	Structure Sensor generated nose bolus	Super-flab ear bolus	CT Reconstructed ear bolus	Structure Sensor generated ear bolus
Dmax (%)	101.10	101.30	102.80	104.30	106.50	107.50
Dmin (%)	94.80	95.00	94.40	93.70	93.60	93.10
Dmean (%)	97.90	98.20	98.90	101.40	103.90	104.10
V95% (%)	100.00	100.00	100.00	100.00	100.00	100.00
D95% (%)	95.90	95.70	96.00	98.60	100.80	100.90
D90% (%)	96.20	96.10	96.50	99.40	101.70	101.70

References

1. Sung H, Ferlay J, Siegel RL, Laversanne M, Soerjomataram I, Jemal A, et al. Global cancer statistics 2020: GLOBOCAN estimates of incidence and mortality worldwide for 36 cancers in 185 countries. CA Cancer J Clin. 2021;71(3):209-49.

2. Bekker RA, Kim S, Pilon-Thomas S, Enderling H. Mathematical modeling of radiotherapy and its impact on tumor interactions with the immune system. Neoplasia. 2022;28:100796.

3. Barazzuol L, Coppes RP, van Luijk P. Prevention and treatment of radiotherapy-induced side effects. Mol Oncol. 2020;14(7):1538-54.

4. Pucci C, Martinelli C, Ciofani G. Innovative approaches for cancer treatment: Current perspectives and new challenges. Ecancermedicalscience. 2019;13:961.

5. Vyas V, Palmer L, Mudge R, Jiang R, Fleck A, Schaly B, et al. On bolus for megavoltage photon and electron radiation therapy. Med Dosim. 2013;38(3):268-73.

6. Zhang C, Lewin W, Cullen A, Thommen D, Hill R. Evaluation of 3D-printed bolus for radiotherapy using megavoltage X-ray beams. Radiol Phys Technol. 2023;16(3):414-21.

7. Park JW, Yea JW. Three-dimensional customized bolus for intensity-modulated radiotherapy in a patient with Kimura's disease involving the auricle. Cancer Radiother. 2016;20(3):205-9.

8. Kudchadker RJ, Antolak JA, Morrison WH, Wong PF, Hogstrom KR. Utilization of custom electron bolus in head and neck radiotherapy. J Appl Clin Med Phys. 2003;4(4):321-33.

9. Kong Y, Yan T, Sun Y, Qian J, Zhou G, Cai S, et al. A dosimetric study on the use of 3D-printed customized boluses in photon therapy: A hydrogel and silica gel study. J Appl Clin Med Phys. 2019;20(1):348-55.

10. Lu Y, Song J, Yao X, An M, Shi Q, Huang X, et al. 3D printing polymer-based bolus used for radiotherapy. Int J Bioprint. 2021;7(4):414.

11. Maxwell SK, Charles PH, Cassim N, Kairn T, Crowe SB. Assessing the fit of 3D printed bolus from CT, optical scanner and photogrammetry methods. Phys Eng Sci Med. 2020;43(2):601-7.

12. Skinner L, Knopp R, Wang YC, Dubrowski P, Bush KK, Limmer A, et al. CT-less electron radiotherapy simulation and planning with a consumer 3D camera. J Appl Clin Med Phys. 2021;22(7):128-36.

13. Baltz GC, Chi PCM, Wong PF, Wang CW, Craft DF, Kry SF, et al. Development and validation of a 3D-printed bolus cap for total scalp irradiation. J Appl Clin Med Phys. 2019;20(3):89-96.

14. Subashi E, Jacobs C, Hood R, Kirsch DG, Craciunescu O. A design process for a 3D printed patient-specific applicator for HDR brachytherapy of the orbit. 3D Print Med. 2020;6(1):15.

15. Gomez G, Baeza M, Mateos JC, Rivas JA, Simon FJL, Ortega DM, et al. A three-dimensional printed customized bolus: Adapting to the shape of the outer ear. Rep Pract Oncol Radiother. 2021;26(2):211-7.

16. Al-Hamad KQ, Al-Rashdan BA, Al-Kaff FT. Virtual patient representation with silicone guide and a 3D scanner accessory for a user-friendly facial scanning workflow: A clinical report of smile design and ceramic veneers. J Prosthet Dent. 2023:S0022-3913(23)00286-X.

17. Burleson S, Baker J, Hsia AT, Xu Z. Use of 3D printers to create a patient-specific 3D bolus for external beam therapy. J Appl Clin Med Phys. 2015;16(3):5247.

18. Dyer BA, Campos DD, Hernandez DD, Wright CL, Perks JR, Lucero SA, et al. Characterization and clinical validation of patient-specific three-

dimensional printed tissue-equivalent bolus for radiotherapy of head and neck malignancies involving skin. Phys Med. 2020;77:138-45.

19. Dahn HM, Boersma LJ, de Ruysscher D, Meattini I, Offersen BV, Pignol JP, et al. The use of bolus in postmastectomy radiation therapy for breast cancer: A systematic review. Crit Rev Oncol Hematol. 2021;163:103391.

20. Wang X, Wang X, Xiang Z, Zeng Y, Liu F, Shao B, et al. The clinical application of 3D-printed boluses in superficial tumor radiotherapy. Front Oncol. 2021;11:698773.

21. Dipasquale G, Poirier A, Sprunger Y, Uiterwijk JWE, Miralbell R. Improving 3D-printing of megavoltage X-rays radiotherapy bolus with surface-scanner. Radiat Oncol. 2018;13(1):203.

22. Park JW, Oh SA, Yea JW, Kang MK. Fabrication of malleable three-dimensional-printed customized bolus using three-dimensional scanner. PLoS One. 2017;12(5):e0177562.

23. Fujimoto K, Shiinoki T, Yuasa Y, Hanazawa H, Shibuya K. Efficacy of patient-specific bolus created using three-dimensional printing technique in photon radiotherapy. Phys Med. 2017;38:1-9.